

AD-A015 943

THRESHOLD LESION TEMPERATURES IN LASER-IRRADIATED  
RABBIT EYES

G. D. Polhamus, et al

Texas University at Austin

Prepared for:

Air Force Office of Scientific Research

31 March 1975

DISTRIBUTED BY:

**NTIS**

National Technical Information Service  
U. S. DEPARTMENT OF COMMERCE



**UNCLASSIFIED**

**SECURITY CLASSIFICATION OF THIS PAGE(When Data Entered)**

(continued)

ture for 30 measurements in 13 rabbits was 54°C. System error was estimated at 5% of temperature rise, or slightly less than 1°C.

ia

**UNCLASSIFIED**

**SECURITY CLASSIFICATION OF THIS PAGE(When Data Entered)**

297094

# Threshold Lesion Temperatures in Laser-Irradiated Rabbit Eyes

ADA015943

by

G. D. Polhamus and A. J. Welch  
Department of Electrical Engineering

Technical Report No. 168  
March 31, 1975

DDC  
RECEIVED  
OCT 1 1975  
C

**BIO-MEDICAL ENGINEERING RESEARCH LABORATORY**

Reproduced by  
NATIONAL TECHNICAL  
INFORMATION SERVICE  
U.S. Department of Commerce  
Springfield, VA. 22151

DISTRIBUTION STATEMENT A  
Approved for public release;  
Distribution Unlimited

**ELECTRONICS RESEARCH CENTER  
THE UNIVERSITY OF TEXAS AT AUSTIN  
Austin, Texas 78712**

The Electronics Research Center at The University of Texas at Austin constitutes interdisciplinary laboratories in which graduate faculty members and graduate candidates from numerous academic disciplines conduct research.

Research conducted for this technical report was supported in part by the Department of Defense's JOINT SERVICES ELECTRONICS PROGRAM (U.S. Army, U.S. Navy, and the U.S. Air Force) through the Research Contract AFOER F44620-71-C-0091. This program is monitored by the Department of Defense's JSEP Technical Advisory Committee consisting of representatives from the U.S. Army Electronics Command, U.S. Army Research Office, Office of Naval Research, and the U.S. Air Force Office of Scientific Research.

Additional support of specific projects by other Federal Agencies, Foundations, and The University of Texas at Austin is acknowledged in footnotes to the appropriate sections.

Reproduction, translation, publication, use and disposal in whole or in part by or for the United States Government is permitted.

Qualified requestors may obtain additional copies from the Defense Documentation Center, all others should apply to the Clearinghouse for Federal Scientific and Technical Information.

ACCESSION TAG	
NTIS	W
DCC	D
UNANNOUNCED	
JUSTIFICATION	
BY _____	
DISTRIBUTION/AVAIL	
Dist.	DATE
A	

THRESHOLD LESION TEMPERATURES IN  
LASER-IRRADIATED RABBIT EYES\*

by

G. D. Polhamus  
A. J. Welch

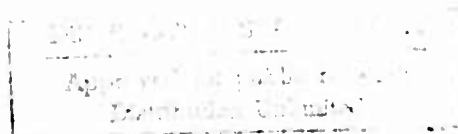
Department of Electrical Engineering

Technical Report No. 168  
March 31, 1975



BIO-MEDICAL ENGINEERING RESEARCH LABORATORY

Electronics Research Center  
The University of Texas at Austin  
Austin, Texas 78712



\*Research sponsored in part by the Joint Services Electronics Program  
under Research Contract F44620-~~77~~<sup>77</sup>-C-0091.

Approved for public release; distribution unlimited.

ib

## ABSTRACT

The purpose of this research was to measure threshold temperatures corresponding to the formation of minimum ophthalmoscopically visible lesions induced in rabbit fundi by a ten-second exposure from an argon C. W. laser (4880Å). The posterior pole of the eye was surgically exposed and a specially designed microthermocouple with a 20-micron diameter tip was inserted into the ocular fundus to measure temperature rises. The mean threshold temperature for 30 measurements in 13 rabbits was 54°C and the standard deviation was 3°C. System error was estimated at 5% of temperature rise, or slightly less than 1°C.

## TABLE OF CONTENTS

		<u>PAGE</u>
	ABSTRACT . . . . .	ii
	LIST OF FIGURES . . . . .	v
Chapter I	INTRODUCTION . . . . .	1
	Discussion of Rate Process Modeling . . . . .	1
	Previous Work . . . . .	3
Chapter II	EXPERIMENTAL PROCEDURE . . . . .	6
	Apparatus . . . . .	6
	Laboratory Procedure . . . . .	8
	Data Analysis . . . . .	11
Chapter III	RESULTS . . . . .	13
	Irradiance Profile. . . . .	13
	Temperature Rise vs. Time . . . . .	14
	Tabulated Data . . . . .	17
	Temperature Rise vs. Fundus Temperature . . . . .	19
	Distribution of Lesions with Threshold Temperature . . . . .	19
	Measured Temperature Rise vs. Calculated Temperature Rise . . . . .	19

<b>Chapter IV</b>	<b>DISCUSSION . . . . .</b>	<b>23</b>
	<b>Sources of Experimental Variation . . . . .</b>	<b>23</b>
	<b>Subthreshold Temperatures . . . . .</b>	<b>25</b>
	<b>Temperature Rise vs. Fundus Temperature . . . . .</b>	<b>26</b>
	<b>Distribution of Lesions with Threshold Temperature . . . . .</b>	<b>26</b>
	<b>Measured vs. Model Temperature Rises . . .</b>	<b>28</b>
<b>Chapter V</b>	<b>CONCLUSIONS . . . . .</b>	<b>30</b>
<b>REFERENCES</b>	<b>. . . . .</b>	<b>31</b>

LIST OF FIGURES

<u>FIGURE</u>		<u>PAGE</u>
1	Experimental Apparatus . . . . .	7
2	Irradiance Profile . . . . .	15
3	Temperature Rise vs. Time . . . . .	16
4	Threshold Temperature Rise vs. Fundus Temperature . . . . .	20
5	Distribution of Lesions with Threshold Temperature . . . . .	21
6	Measured Temperature Rise vs. Calculated Temperature Rise . . . . .	22

## CHAPTER I

### INTRODUCTION

The research reported in this report concerns the measurement of threshold temperatures associated with retinal injury due to local laser-induced ophthalmoscopically visible fundus changes. These threshold temperatures are critical to the development of a model that describes the process of thermal damage in the fundus. Henriques has assumed that damage results from protein denaturation and has used Arrhenius' equation to model cutaneous thermal damage by a rate process in which parameters were evaluated with blister threshold temperatures. Although the rate process of thermal damage due to protein denaturation is generally accepted, [Fugitt, 1955; Stoll, 1959; Hu and Barnes, 1970], there exists data for rejecting this hypothesis [Vassilidis, 1971; Priebe, Cain and Welch, unpublished].

#### Discussion of Rate Process Modeling

Rate process models for thermal tissue damage have been based on the following equation:

$$\frac{ds}{dt} = K's$$

in which

$s$  = surviving fraction of biomaterial

$K'$  = reactions rate coefficient

$$= \frac{kT}{h} \exp\left(-\frac{\Delta H - T \Delta S}{RT}\right)$$

where

$\Delta H$  = change in heat energy

$\Delta S$  = change in entropy

$T$  = temperature in  $^{\circ}\text{K}$

$k$  = Boltzmann's constant in CGS

$h$  = Planck's

$R$  = Universal gas constant =  $2.0 \text{ cal}/^{\circ}\text{K}/\text{mol}$

During early modeling attempts, temperature was assumed constant and the equation had the following simple form:

$$\Omega = P e^{\Delta E/RT_t}$$

where

$\Omega$  = tissue damage

$P$  = integration constant

$E$  = energy of activation

$r$  = gas constant

$T$  = tissue temperature

$t$  = exposure time.

In general  $\Omega$  was arbitrarily assumed equal to unity for threshold damage, and  $P$  and  $E$  were then determined empirically from the data. However, using the more specific form of the equation, a critical

temperature ( $T_c$ ) can be calculated for which the original material will be reduced by  $1/e$ .

$$T_c = \frac{\Delta H}{58.6 + \Delta S = 4.56 \log_{10} t'}$$

where  $t'$  = length of temperature pulse.

Proper selection of  $\Delta H$  and  $\Delta S$  will allow the definition of a critical temperature for retinal damage, after which it should be possible to completely define the geometry of a lesion. Selection of these values has, unfortunately, proved troublesome. However, the recording of threshold temperatures for damage at each individual retinal layer, and correlation between these temperatures and histologically determined lesion geometries will hopefully provide further insight into the definition of the appropriate model and associated parameters involved for retinal damage.

### Previous Work

Numerous authors have used wire thermocouples to measure fundus temperatures [Mellerio, 1966; Najac, 1963; Noyori, 1963], but their results have been questioned [Geeraets, et. al., 1963; Vos, 1966; Hays and Wolbarsht, 1968]. Recent measurements of fundus temperature have been by Cain and Welch, who measured laser-induced fundus temperature changes with 20-micron diameter quartz thermocouples [Cain and Welch, 1974]. These probes have been specifically designed for measuring temperature transients in tissue [Cain and Welch, 1972;

Reed, 1966]. Cain and Welch have shown experimentally that probe artifact may be minimized by maintaining a 10 to 1 ratio between retinal image half-power diameter and probe diameter. Although they measured complete temperature-time histories in the laser-irradiated fundus, Cain and Welch did not measure temperatures at which minimum ophthalmoscopically visible fundus changes occurred. They used a model developed by White, et al to predict temperature rises in their experiments [White, et al, 1970]. The model was based on a finite difference (ADI technique) solution of the heat conduction equation in cylindrical coordinates:

$$\nabla \cdot (k \nabla T) + A = \rho c \frac{\partial T}{\partial t}$$

in which

- T = absolute temperature or temperature rise
- k = thermal conductivity in cal/cm sec °C
- A = heat source term in cal/cm<sup>3</sup> sec
- $\rho c$  = volumetric specific heat in cal/cm<sup>3</sup> °C
- c = specific heat in cal/gm °C
- $\rho$  = density in gm/cm<sup>3</sup>.

Exponential absorption was assumed for the pigment epithelium (P.E.) and choroid, the retinal image was assumed circularly symmetric and the ocular media was assumed thermally homogenous and isotropic within each layer. Experimental input data to the model included corneal power, image radius, and relative irradiance profile at the retina.

(energy distribution). Other input parameters to the model were transmission of the ocular media, thickness and absorption coefficients of the P.E. and choroid, and conductivity and volumetric specific heat for each layer.

The temperature sensors were made from 1 mm quartz rod pulled over heat to 20 microns diameter at the tip. Nickel, parylene (insulation) and copper were deposited on the quartz substrate, allowing a copper-nickel junction only at the probe tip. Thermoelectric EMF was  $21 \mu V/^{\circ}C (\pm 1 \mu V/^{\circ}C)$  and rise time to 90% of equilibrium was about 1 msec. for a near step change in temperature produced by driving a probe into a heated water bath.

This report presents laser-induced threshold temperatures obtained with the quartz probes for retinal image half power diameters of approximately 200 to 400 microns in the ocular fundi of rabbits. The report shall (1) detail the experimental procedure used to obtain threshold temperatures, (2) graphically present the results, (3) discuss the results and (4) offer conclusions to be drawn from these results. Much of the experimental procedure is identical to that followed by Cain and Welch, and for details beyond those mentioned in this report, the reader is referred to their publications [Cain and Welch, 1972; Cain and Welch, 1974].

## CHAPTER II

### EXPERIMENTAL PROCEDURE

This chapter includes a description of the apparatus, an outline of the laboratory procedure and mention of the data analysis.

#### Apparatus

The physical location of the experimental apparatus used in this research is shown in Fig. 1. The temperature-sensing probes were produced in the Engineering Research Laboratory at The University of Texas at Austin, under the supervision of Professor E. A. Ripperger. A detailed description of the probe manufacturing process and its properties can be found elsewhere [Cain and Welch, 1972].

The sensor output first entered a specially made preamplifier which had a gain of 1000 and a bandwidth from DC to 10 kHz. The amplified signal was displayed on a Clevite Brush Mark 200 8-channel strip chart recorder with bandwidth of DC to 100 Hz. The overall bandwidth of the system was about 90 Hz. To insure that critical information was not being inadvertently filtered, several temperature rises were recorded on a Sangamo 3500, 14-channel magnetic tape recorder with record and playback speeds capable of scaling time by a factor of 32.

Prior to each experiment, the temperatures sensor was calibrated to (a) assure the EMF of a sensor was within acceptable limits ( $\pm 1 \mu V/^{\circ}C$ ) of  $21 \mu V/^{\circ}C$ , and (b) verify the system's integrity.

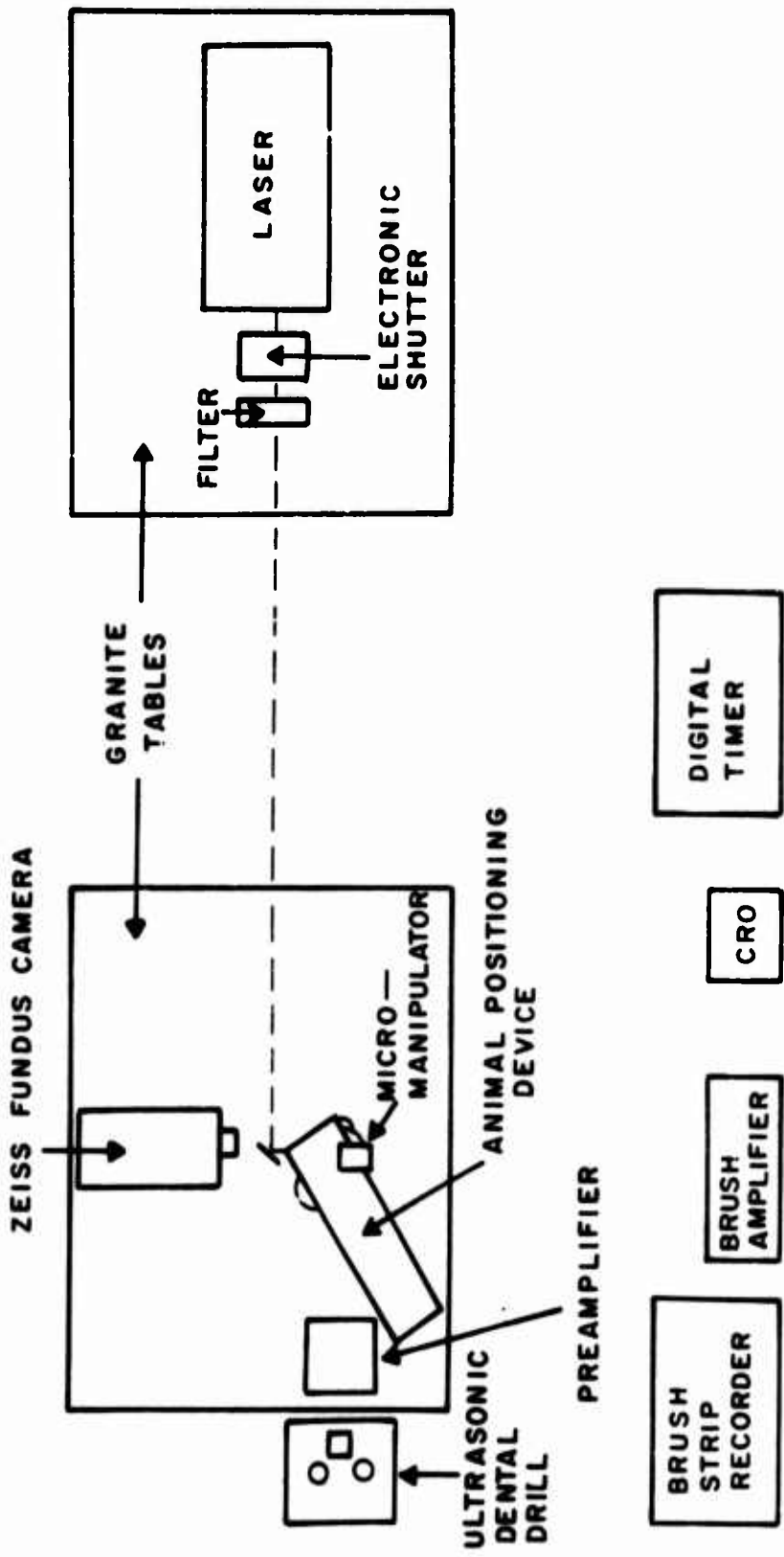


Figure 1. Experimental Apparatus.

The eye was irradiated by a Spectra-Physics Model 166-03 argon-ion laser, tuned to a primary wavelength of  $4880\overset{\circ}{\text{Å}}$ . Pulse length was controlled with an electronic shutter, from Vincent Associates, Model 23XDB2X5, in conjunction with a Devices Sales Ltd. digital timer. The ocular fundus was viewed with a Zeiss Fundus Camera. Mounted immediately beyond the fundus camera lens was a beam splitter to allow viewing of the fundus while half the energy from the argon laser was directed into the eye. The fundus camera was used to observe image location and lesion formation on the fundus.

Radiant energy was measured with an EG & G Model 580 Radiometer with a narrow beam adapter and 25A Detector Head. Neutral density filters were placed in the laser beam path to control intensity.

### Laboratory Procedure

The laboratory procedure is divided into two portions:

(1) Surgical Procedure and Sensor Insertion, and (2) Temperature Measurement.

(1) Surgical Procedure and Sensor Insertion. Thorough documentation already exists for the surgical procedure used in this experiment [Cain and Welch, 1972]. The rabbit was anesthetized with sodium pentobarbital, Nembutal. Then a tracheostomy was performed and the animal was maintained on positive respiration for the remainder of the experiment. The animal was affixed on the animal positioning device with ear bars and a mouthpiece. The sclera was exposed by excision of the

supraorbital process of the frontal bone from anterior to posterior projection, followed by excision of the Levator Palpebrae muscle, Superior Rectus muscle, and partial excision of the lacrimal gland and Harder's gland. In general, cauterization was necessary to control hemorrhaging. Six sutures were placed through the conjunctiva and the eyeholder was sewn onto the front of the eye. A contact lens was used to keep the cornea moist.

Preceding the insertion of the fragile 20-micron diameter sensor into the ocular fundus, a 3-micron drill probe was used to pierce the sclera. These drill probes were usually 1 mm quartz rods, pulled over heat, tapering quickly down to a tip a couple microns in diameter. The probes were mounted in a Cavitron Model C210 Ultrasonic Dental Drill affixed to a Narishigi Hydraulic Micromanipulator, with which they were propelled through the sclera. The drill probe was then replaced by the temperature sensor, and the insertion completed. Occasionally, local tissue trauma due to the insertion could be observed, which sometimes caused hemorrhaging at the insertion site. Such sites were always abandoned.

(2) Temperature Measurements. During the course of the experiments several variables were constantly monitored. The ECG and pain reflex to pinching between the toes allowed fair estimation of the animal's general state of health and anesthesia. Once the temperature sensor was inserted into the fundus, steady-state temperature of the eye was monitored. Body temperature and tissue temperature at the back of the eye were monitored

in most of the experiments. A Sears Heat Lamp was used to keep fundus temperature near  $37^{\circ}\text{C}$ .

Once the temperature sensor was in position, the following steps were taken:

(a) The probe tip was moved into the vitreous (to minimize conduction effects), and 5 msec. laser pulses were applied to the eye. The animal was rotated until the probe was in the center of the image (presumably the point of maximum direct absorption for the sensor). A relative intensity distribution of the retinal image was obtained by rotating the animal about the center of the ocular lens system by precise increments, and measuring the direct temperature rise produced by a 5-msec. pulse at each increment. Rotation about the center of the lens system resulted in minimal movement of the image in space, as the fundus, and inserted sensor, moved across it. The profile was assumed circularly symmetric.

It has been shown that to adequately reduce the temperature response error introduced by the presence of the probe in the ocular media, the half-power diameter of the retinal image must be 10 times the probe diameter. [Gain and Welch, 1972]. To obtain this condition, a 30 cm focal length lens was placed in the laser beam path to provide a near Maxwellian View to the rabbit eye (i.e., the laser beam was focused near the center of the animal's lens system).

(b) Locations near the sensor insertion (within 1 mm) were irradiated at decreasing power levels for ten-second intervals, until a

certain power was associated with a minimum ophthalmoscopically visible fundus change appearing within five minutes after exposure. The animal was then moved to impinge the laser upon the insertion site, and short 50 msec. pulses were applied while sensor position was adjusted until the location of maximum temperature rise was achieved. Then a ten-second pulse at about one-fourth the power necessary for a threshold lesion was applied and temperature rise was recorded on the Brush Recorder. The sensor was repositioned to remedy any movement of the animal or shift of the image, and this subthreshold temperature was again recorded. Finally, the sensor was repositioned once more and full threshold power was delivered to the site. It has been reported that rates of tissue damage are negligible when subthreshold temperatures are kept below reasonable levels [Stoll, 1959; Hu and Barnes, 1970]. All experimental subthreshold temperature rises were kept below  $8^{\circ}\text{C}$ .

(c) A few times it was possible to begin afresh, and reinsert the sensor at a new location, and repeat the entire experiment.

### Data Analysis

Several steps were necessary to reduce the data to a meaningful form. First, the temperature rise due to direct absorption by the sensor was subtracted from the overall recorded temperature rise. The remainder represented the tissue temperature rise. The rapid response of the sensor, due to direct heating, was easily differentiable from the response due to the slower heating of the tissue.

Second, the temperature rises associated with the subthreshold laser pulses were linearly extrapolated to the threshold corneal power to obtain the temperature rise associated with threshold corneal power.

$$T_t^e = \frac{T_s^m \times CP_t}{CP_s}$$

in which

$T_t^e$  = extrapolated temperature rise associated with threshold corneal power

$T_s^m$  = measured subthreshold temperature rise

$CP_s$  = subthreshold corneal power

$CP_t$  = threshold corneal power.

The validity of a linear relation between corneal power and temperature in the ocular fundus has been established [Cain and Welch, 1974; Priebe, Cain and Welch, unpublished].

A least-squares curve fit was applied to the data (threshold temperature rise vs. fundus temperature) and the coefficients of the fit then used to correct all data to a fundus temperature of 37°C. The mean, standard deviation and 95% confidence intervals for the corrected temperature rise were then computed.

Finally, the relation between model temperatures and measured temperatures was examined by a least-squares curve fit between these two variables.

## CHAPTER III

### RESULTS

Data were taken from twenty rabbits, three of which had two sensor insertions and a fourth of which had three insertions. In addition to threshold measurements, subthreshold measurements were obtained from nine of these rabbits (including two of the double insertions and the triple insertion). These subthreshold measurements were extrapolated to threshold temperatures. A total of thirty-eight measured or extrapolated threshold temperatures were obtained during this research. Only thirty values have been selected for presentation. The others have been discarded for various reasons, such as excessive variation in pre-lesion fundus temperature from  $37^{\circ}\text{C}$ , apparent degradation of corneal clarity, or excessive localized trauma from inserting the probe.

The experimental results have been summarized in a set of figures and tables. The presented data includes a sample irradiance profile and temperature response profile, plots of threshold temperature rise vs. fundus temperature, distribution of lesions with threshold temperature, and calculated threshold temperature vs. measured threshold temperature rise.

#### Irradiance Profile

The computer solution to the heat conduction equation uses the shape of the heat source at the fundus as one of its input parameters. Hence, for every experiment, the direct heating characteristic of the sensor

was used to measure the irradiance profile at the retina. This is a profile of the laser image intensity at the fundus. An example of the irradiance profile is shown in Fig. 2 for experiment 25A. System noise prevented measurements below 10% of the profile maximum. Retinal image diameter which is required for the temperature calculation, was always assumed to be twice the distance from image center to the smallest discernible absorptive temperature rise above minimum noise. The dashed portion of the smooth line drawn through the experimental points, indicates the region of measurement uncertainty. Half-power image diameter at the fundus for this particular experiment was about 210 microns, which is a typical value. The circular symmetric profile used by the model was achieved by averaging of both sides of the profile in Fig. 2.

#### Temperature Rise vs. Time

The measured and calculated (from the model) temperature rises in the P.E. at the center of the beam as a function of time for rabbit 25A are shown in Fig. 3. The 13.8 mW (at cornea) laser pulse produced a retinal image with half-power diameter of 210 microns. The duration of the exposure was 10 seconds. Maximum measured temperature rise was  $17.6^{\circ}\text{C}$  and maximum model temperature rise was  $16.5^{\circ}\text{C}$ . Again, a smooth line has been drawn through the points. The initial portion of the model profile lies above the measured profile. However, the curves cross at about one second, and thereafter, the model profile remains lower than

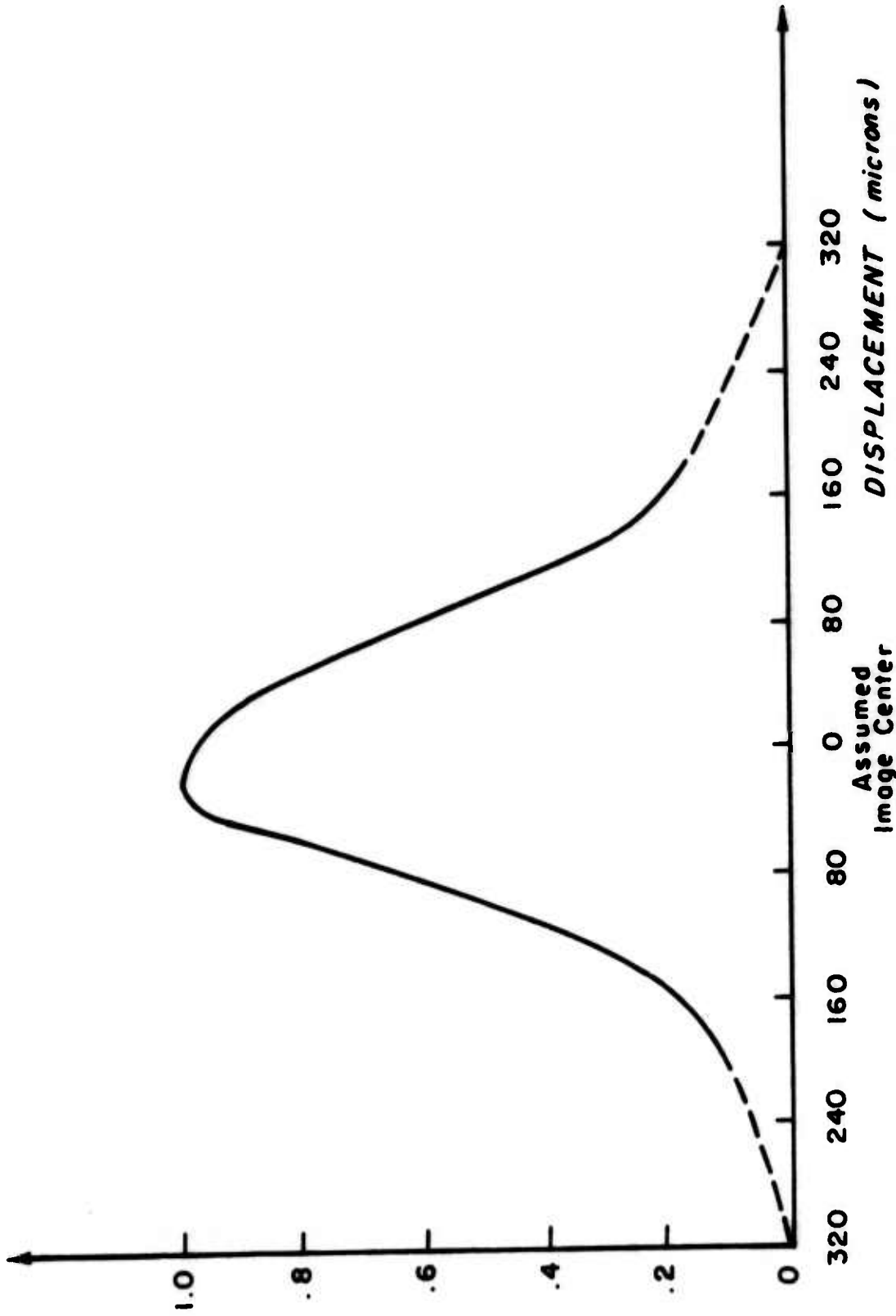


**Figure 2.** Irradiance Profile.  
Energy Distribution Measured At Retina From  
Experiment 25A. (Dashed lines indicate region  
of uncertainty).

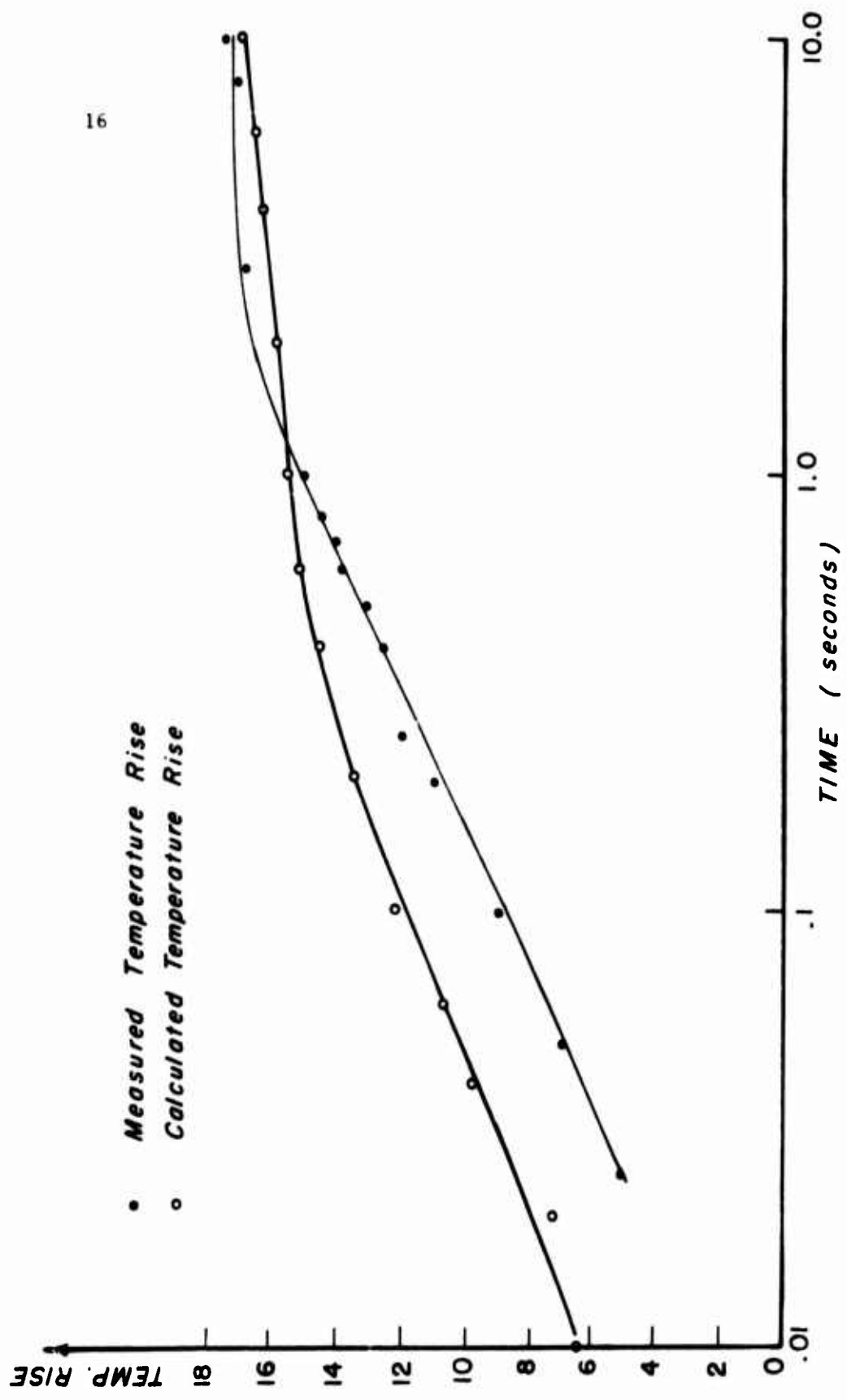


Figure 3. Temperature Rise vs. Time .  
Temperature-Time Profile for Experiment 25A

the measured profile. At the end of the laser pulse, the measured temperature has stabilized. However, the model temperature increases at a slow rate.

### Tabulated Data

Table I is a list of thirty threshold burn temperatures from twenty rabbits. The pre-lesion fundus temperature and temperature rises calculated by the model are also listed.

Parameters used for these calculations were as follows: Thicknesses of the P.E. and choroid were assumed to be 10 and 100 microns, respectively. Absorption coefficients for 4880Å of 832.0 and 83.2 cm<sup>-1</sup> were used for the P.E. and choroid, respectively. Pre-retinal ocular media transmission was assumed to be 82.0% for the aforementioned wavelength. Conductivity (k) and volumetric specific heat (ρc) were specified as 0.0015 Cal/°C sec. cm. and 1.0 Cal/°C cm<sup>3</sup>, respectively, for each layer. Both the absorption coefficients and the pre-retinal ocular media transmission were higher than the values used by Cain and Welch [Cain and Welch, 1974]. For their calculations, absorption coefficients were 637.6 cm<sup>-1</sup> and 76.3 cm<sup>-1</sup> for the P.E. and choroid, respectively, and transmission of the ocular media was 63.6%.

Half-power image diameters were always kept between 200 microns and 400 microns. All lesions were produced by ten-second laser pulses.

Table 1. Results

Experiment	Fundus Temperature (°C)	Corneal Power (mW)	1/2-Power Image Diameter (microns)	Energy Density (Joule/cm <sup>2</sup> )	Temperature Rise (°C)		Threshold Temperature (°C)	
					Measured	Extrapolated From Measured Sub-Threshold	Measured	Extrapolated From Measured Sub-Threshold
7	35*	41	240	457.	17	-	38.9	52.
10	35*	19	360	112.	16	-	14.4	51.
12	35*	21.6	280	187.	16.75	-	19.5	51.25
13a	32.25*	20.	200	304.	21.75	-	22.3	54.
13b	33.5*	20.	200	304.	23.	-	22.3	56.5
14	35.	19.	280	193.	19.5	-	17.8	59.5
16	35.	26.	210	524.	18.	26.9	35.3	52.5
18a	31.5	31.	260	239.	20.5	24.9	23.5	52.
18b	31.5	26.	320	187.	23.	24.9	21.3	54.5
19	38.3	20.	400	86.3	18.	19	12.7	56.3
20a	36.7	22.	360	150.	11.5	17.9	16.6	48.2
20b	36.	22.	360	150.	14.	17.9	16.6	50.
22	37.5	19.0	200	434.	20.	20.4	25.3	57.5
23	40.	16.6	240	245.	13.5	13.9	18.5	53.5
24	41.5	19.5	300	145.	13.2	20.1	15.4	54.7
25a	37.	13.8	210	223.	17.6	16.8	16.5	54.6
25b	37.5	18.	200	237.	19.25	20.9	20.	56.75
25c	44.5	6.8	180	115.	6.0	6.8	8.5	50.5

\* Fundus temperature assumed 2°C lower than body temperature

### Temperature Rise vs. Fundus Temperature

Extrapolated and measured threshold temperature rises are presented as a function of pre-lesion fundus temperature in Fig. 4. Minimum and maximum fundus temperatures were  $31.5^{\circ}\text{C}$  and  $44.5^{\circ}\text{C}$ , respectively. A straight line of slope  $-1.05$  and  $y$ -intercept  $56^{\circ}\text{C}$  which was obtained by a least-squares curve fit has been drawn through the data. Threshold temperatures determined by extrapolation of subthreshold temperatures are depicted by open circles.

### Distribution of Lesions with Threshold Temperature

Figure 5 is an accumulation of the number of experimental lesions as a function of increasing threshold temperatures (steady-state fundus temperature plus measured temperature rise). All thirty lesions appear in this graph. Only one lesion appears at  $48.2^{\circ}\text{C}$  and 15 lesions appear at  $54.5^{\circ}\text{C}$  or lower. Temperature interval is  $2^{\circ}\text{C}$ . A smooth line is drawn through the points.

### Measured Temperature Rise vs. Calculated Temperature Rise

The relation between measured temperature rises and calculated temperature rises is shown in Fig. 6. Calculated temperatures are based on experimentally measured corneal power, irradiance profile and image radius. A straight line of slope  $0.92$  (from least-squares curve fit) has been drawn through the data. Again, extrapolated threshold temperatures have been depicted by open circles.

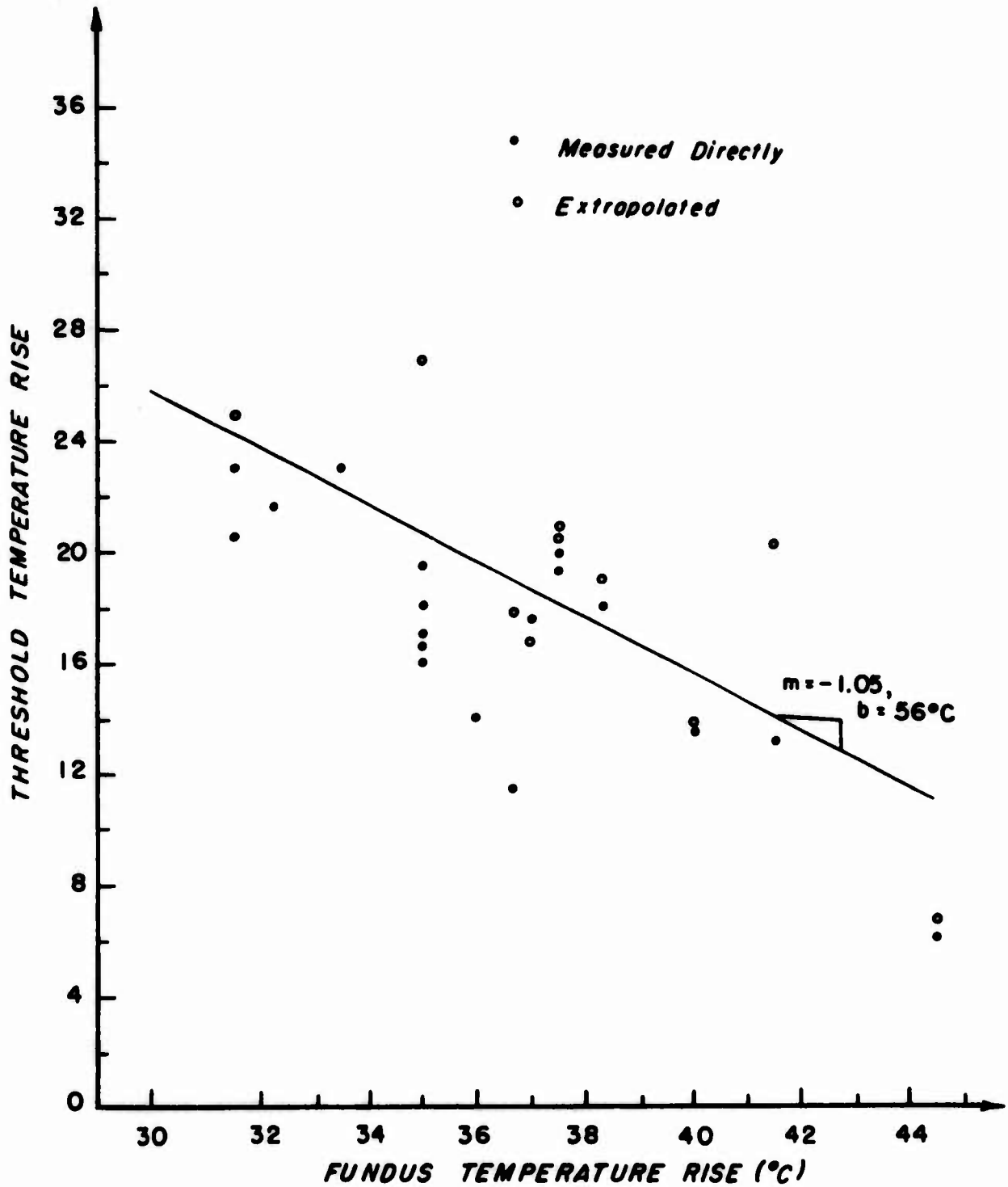


**Figure 4.** Threshold Temperature Rise vs. Fundus Temperature.

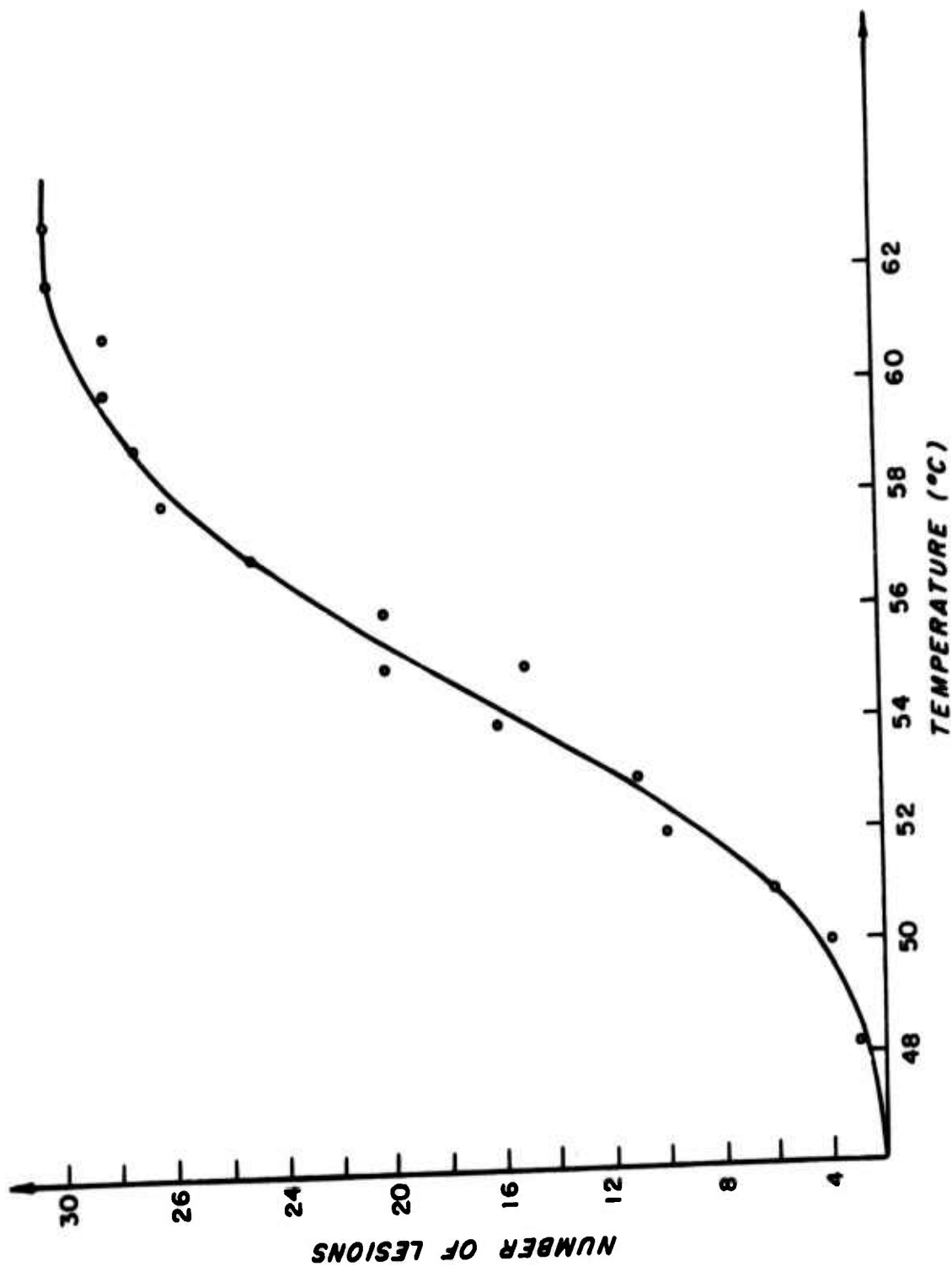
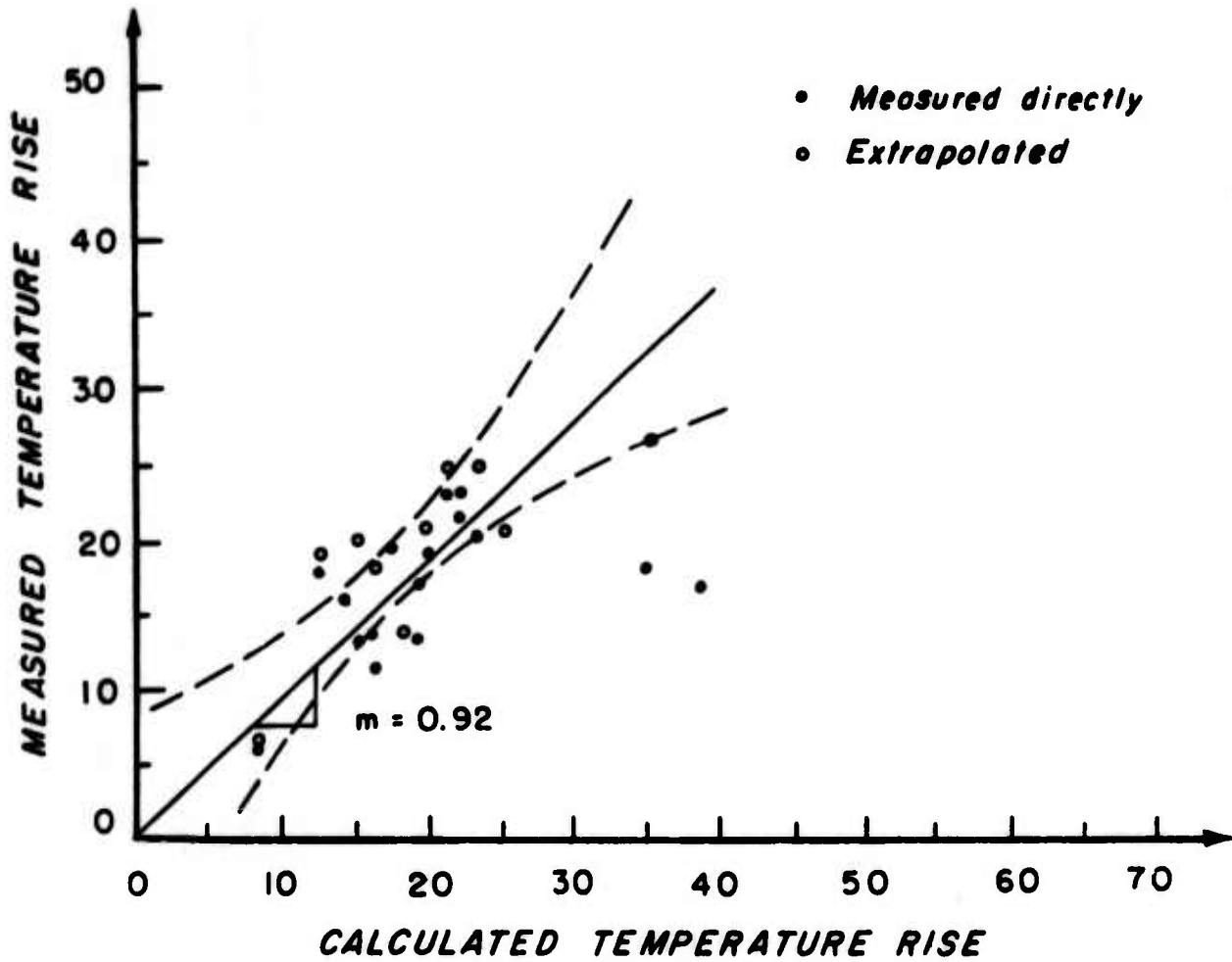


Figure 5. Distribution of Lesions with Threshold Temperature



**Figure 6.** Measured Temperature Rise vs. Calculated Temperature Rise. Dashed lines indicate 95% confidence band for slope  $m = 1$ .

## CHAPTER IV

### DISCUSSION

The results shall be discussed with respect to the following five topics: (1) Sources of Experimental Variation, (2) Subthreshold Temperatures, (3) Temperature Rise versus Fundus Temperature, (4) Number of Lesions versus Temperature, and (5) Measured Temperature versus Calculated Temperature.

#### Sources of Experimental Variation

A number of potential sources of experimental variation exist for these experiments. Most of these are associated with the system and procedure used to measure retinal temperature; however, some sources of variation appear to be inherent in the phenomena responsible for lesion formation.

Many of the possible sources of system variation have been analyzed elsewhere [Cain and Welch, 1972]. Near steady-state temperatures have been reported with an accuracy of approximately  $\pm 5\%$  (including the variation of  $\pm 0.5^{\circ}\text{C}$  introduced by system calibration and  $\pm 0.5^{\circ}\text{C}$  from subtraction of the direct absorption component).

The use of an invasive technique to measure fundus temperatures immediately raises questions regarding the effect of the probe's presence in the tissue. The thermal resistance between the probe and the tissue is assumed negligible, which is reasonable since (1) the width of

such an interface resistance is small, thus reducing its contribution; and (2) thermal properties of the biomedica composing the interface resistance would be similar to those of the ocular tissue. Of course, the presence of the probe introduces an anomaly into the conducting field, unequivocally affecting the axial and radial heat fluxes. However, as mentioned earlier, Reed has shown that this effect should be minimized by the use of a sensor material that has properties of thermal conductivity ( $k$ ) and volumetric specific heat ( $\rho c$ ) such that  $k/\rho c$  and  $k\rho c$  each approximately equal 0.00144 ( $k\rho c_{H_2O} = k/\rho c_{H_2O} = 0.00144$ ). For comparison, the thermal parameters for copper are  $k\rho c = 0.76$  and  $k/\rho c = 1.14$ , whereas, the thermal properties for fused quartz are  $k\rho c = 0.00131$  and  $k/\rho c = 0.0083$ . However, the probe's presence in the tissue may produce an even more profound effect on threshold temperature by altering the shape of the heat source. This is caused not only by the high absorptivity of the probe (resulting in high temperatures near the probe), but also by the shadow cast by the opaque probe (resulting in lower temperatures behind the probe). Cain and Welch have shown that keeping the half-power image diameter to probe diameter ratio above 10 to 1 reduces these effects of the probe. Finally, introducing a probe into living tissue must modify the local circulation, though the extent of this modification is uncertain. Again, confidence in neglecting the effect from this modification is based upon the maintenance of a large retinal image relative to the probe diameter, and the relatively avascular nature of the retinal layers.

Several sources of variation appear to be inherent in the living system. It is well known that the rabbit fundus is not uniform [Clarke, 1970]. During one experiment, a given corneal power could produce a lesion at one retinal location, but not at another approximately 2 mm away. As much as a four to one difference in pigmentation was previously observed in dark-eyed rabbits [Marshall, 1970]. Hopefully, gross variation was prevented by subjective evaluation of pigmentation of each animal.

#### Subthreshold Temperatures

As previously described, two subthreshold temperatures were measured at each sensor insertion site prior to the concluding threshold exposure. Repositioning of the sensor between each exposure helped determine what percentage of the experimental variation was due to failure of the sensor to be placed at the hottest location in the fundus, or to remain at that location.

Generally, one out of every four subthreshold measurements was lower than the other subthreshold measurement at that site. However, this difference, even when extrapolated to threshold corneal power, was rarely more than  $1^{\circ}\text{C}$ . In all cases, the highest of the subthreshold temperatures from each site was selected as the threshold temperature.

### Temperature Rise vs. Fundus Temperature

Threshold temperature rise and pre-lesion fundus temperature appeared to be linearly related (see Fig. 4). Error was probably introduced by using the coefficients from a linear curve fit to correct all data to  $37^{\circ}\text{C}$  for calculating mean and variance. The amount of error introduced and a more appropriate method of correlation, consistent with rate process theory, will hopefully be defined by more extensive threshold studies over wider temperature ranges.

The mean of the threshold temperature rises, after correction to  $37^{\circ}\text{C}$ , was  $17.3^{\circ}\text{C}$  and the standard deviation was  $3.1^{\circ}\text{C}$  or 18% of the mean. Ninety-five percent confidence intervals for the sample mean were  $\pm 1.2^{\circ}\text{C}$ .

### Distribution of Lesions with Threshold Temperature

One may infer from the relation between the number of lesions appearing and temperature (see Fig. 5), that no obvious skewing of the data occurred. The threshold temperature mean was  $54^{\circ}\text{C}$ .

It is instructive to examine the variance in corneal power necessary for lesion formation, and compare to the variance of the temperature measurements. Unfortunately, there were only 18 threshold corneal power measurements since extrapolated threshold temperature rises were determined using threshold corneal power. Hence, for all experiments in which subthreshold measurements were taken, a single threshold corneal

power was associated with both the measured threshold temperature rise and the extrapolated temperature rise. Nevertheless, the mean of these 18-corneal power measurements was 21.3 mW, and the standard deviation was 6.86 mW or about 32% of the mean.

Data are also available from other laboratory sources. An argon laser (4880Å) has been used to produce damage in the rhesus monkey retina, which is presumably more uniform than the rabbit retina [Vassiliadis, et. al., 1969]. In those experiments, exposure time was 1600 msec. and retina spot size was about 200 microns. The mean was 30 mJ and the standard deviation was about 11 mJ, or 36% of the mean.

The difference in variation between threshold corneal power measurements and threshold temperature measurements suggests that threshold temperatures are somewhat less sensitive to individual physiological differences (i.e., pigmentation, local circulation, and transmission and absorption properties of various ocular components).

It is well known that these minimum ophthalmoscopically visible lesions are probably 10 to 15 percent beyond the first histologically and electroretinographically noticeable permanent alterations [Ham, et. al., 1969; Priebe and Welch, 1972]. Nevertheless, the small variation in threshold temperatures does emphasize the probable correlation between a specific degree of damage and a given temperature and exposure time.

### Measured vs. Model Temperature Rises

The model parameters used for these calculations resulted in temperature rises that averaged about 8% higher than the measured temperature rises. However, the calculated temperature rises averaged only 0.4% higher than the measured temperature rises, when two data points were deleted. The line of slope  $m = 0.92$  lies within the 95% confidence bands for a slope  $m = 1$ , thus encouraging confidence in the predictive power of the model.

In comparison, Cain and Welch obtained measured temperature rises about 20% higher than calculated temperature rises (using different model parameters). Cain and Welch's parameters probably produced better agreement during early exposure times (less than 100 msec.). Unfortunately, short-time temperatures for this research were attenuated by the DC to 90 Hz system bandwidth of the Brush Recorder, and, hence, shall not be compared to Cain and Welch's data.

Calculated temperature rises were subject to variation from many sources. First, variation was induced by assuming the image was circularly symmetric. At best, only a horizontal profile of the laser image at the retina was obtained. Unsymmetric profiles were merely averaged to symmetry. Second, variation resulted from the profile sampling technique of rotating the animal about the center of its lens system while assuming the laser image remained fixed in space. Occasional disagreement between distances across the retina measured with a fundus camera

graticule versus the animal rotation technique suggests a possible under-estimation of this variation at  $\pm 5\%$  [Cain and Welch, 1972]. This variation is due directly to the variation in (1) the distance between the lens and retina, and (2) diopter strength of the lens system. Third, since the image profile (recorded by direct absorption of the sensor) was generally lost in system noise below about 10% of maximum, the retinal image diameter was assumed to be twice the length between the image maximum and 10% of maximum. Under this assumption, the retinal image was somewhat larger than that used for the model calculations. This smaller model profile was assumed to contain the energy of the actual profile, thus tending to produce higher calculated temperature rises. Since energy in the tails of the profile generally was less than 6%, the contribution from this variation was neglected.

Perhaps the most important factor that contributed to a consistent bias to steady-state model temperature rise was the value used for the transmission through the ocular media. The particular wavelength used in this research ( $4880\overset{\circ}{\text{A}}$ ) was close to the lower cut-off wavelength for transmission [Geeraets and Berry, 1968; Mainster et. al., 1969]. Hence, it was difficult to accurately determine this parameter from most ocular transmission charts.

## CHAPTER V

### CONCLUSIONS

The following conclusions may be drawn from this research:

(1) Threshold temperatures, measured by specially designed microthermocouples, have been associated with the formation of minimum ophthalmoscopically visible lesions produced in rabbit fundi by a ten-second exposure from an argon C. W. laser ( $4880\text{\AA}$ ). The mean threshold temperature was  $54^{\circ}\text{C}$  and the standard deviation was  $3^{\circ}\text{C}$ . System error was about 5% of temperature rise or slightly less than  $1^{\circ}\text{C}$ .

(2) Measured threshold temperature rises increased as pre-exposure fundus temperatures decreased. Consequently, threshold temperature appeared to remain constant, within a moderate range of pre-exposure fundus temperatures.

(3) Calculated threshold temperature rises were 0.4% higher than measured steady-state threshold temperature rises, following deletion of two data points.

(4) Threshold temperatures showed better correlation with lesion formation than threshold corneal powers.

(5) The next important step in this research is the examination of a rate process model for thermal damage and the definition of the correlation between exposure, temperature rise and lesion formation.

## REFERENCES

- Fugitt, G. H., "A Rate Process Theory of Thermal Injury," AFSWP-606, USA Special Weapons Project, Washington, D. C., 1955.
- Stoll, A. M., and L. C. Greene, "Relationship Between Pain and Tissue Damage Due to Thermal Radiation," J. Appl. Physiol., Vol. 14, No. 3, May, 1959, p. 373.
- Hu, C., and F. S. Barnes, "The Thermal-Chemical Damage in Biological Material under Laser Irradiation," IEEE Trans. Bio-Med. Engr., Vol. BME-17, No. 3, July, 1970, p. 220.
- Vassiliadis, A., et. al., "Ocular Laser Threshold Investigations," Report No. 8209, Jan., 1971, pp. 35-43.
- Priebe, L. A., and A. J. Welch, Bio-Medical Engineering Laboratories, ENS 612, The University of Texas at Austin, Austin, Texas, 78712.
- Mellerio, J., "The Thermal Nature of Retinal Laser Photocoagulation," Exptl. Eye Res., Vol. 5, p. 242, 1966.
- Najac, H., et. al., "Direct Thermocouple Measurements of Temperature Rise and Heat Conduction in the Rabbit Retina," Invest. Ophth., Vol. 2(1), 1963, p. 32.
- Noyori, K. S., et. al., "Ocular Thermal Effects Produced by Photocoagulation," Arch. Ophth., Vol. 70, 1963, p. 817.
- Geeraets, W. J., and D. Ridgeway, "Retinal Damage from High Intensity Light," Acta Ophth. Suppl. 76, 1963, p. 109.
- Vos, J. J., "Heat Damage to the Retina by Lasers and Photocoagulators," Ophth. Vol. 151, 1966, p. 652.
- Hayes, J. R., and M. L. Wolbarsht, "Thermal Model for Retinal Damage Induced by Pulsed Lasers," Aerospace Med., May, 1968, p. 474.
- Cain, C. P., and A. J. Welch, "Measured and Predicted Laser Induced Temperature Rise in the Rabbit Fundus," Invest. Ophth., Vol. 13, 1974, p. 60.

- Reed, R. P., "Thin Film Sensors of Micron Size and Applications in Biothermology," Ph.D. Dissertation, The University of Texas at Austin, 1966.
- White, T. J., et. al., "Chorioretinal Thermal Behavior," Bull. Math. Bio-physics, Vol. 32, 1970, p. 315.
- Cain, C. P., and A. J. Welch, "Dynamic Spatio-Temporal Temperature Measurements in Laser Irradiated Rabbit Eyes," Report No. 138, Sept. 1972.
- Clarke, A. M., "Ocular Hazards from Lasers and Other Optical Sources," CRC Critical Reviews in Environmental Control, Nov., 1970, p. 307.
- Marshall, J., "Thermal and Mechanical Mechanisms in Laser Damage to the Retina," Invest. Ophth., Vol. 9, No. 2, Feb., 1970, p. 97.
- Vassiliadis, A. et. al., "Research on Ocular Laser Thresholds," Report 7191, Aug., 1969, p. 34.
- Ham, W. T., Jr., et. al., "Effects of Laser Radiation on the Mammalian Eye," Trans. N. Y. Acad. of Sciences. Ser. II, Vol. 28, No. 4, Feb., 1966, p. 517.
- Priebe, L. A., and A. J. Welch, "Changes in the Rabbit Electroretinogram C-Wave Following Ruby Laser Insult," Aerospace Med., Vol. 44, No. 11, Nov., 1973, p. 1246.
- Geeraets, W. J., and E. R. Berry, "Ocular Spectral Characteristics as Related to Hazards from Lasers and Other Light Sources," Amer. J. of Ophth., Vol. 66, No. 1, 1968, p. 15.
- White, T. J., et. al., "Retinal-Temperature Increases Produced by Intense Light Sources," J. Optic. Soc. Am., Vol. 60, No. 2, Feb., 1970, p. 264.
- Henriques, F. C., Jr., "Studies of Thermal Injury," Arch. Path., Vol. 43, 1947, p. 489.